Supporting Information: Opposing Roles for Serotonin in Cholinergic Neurons of the Ventral and the Dorsal Striatum

Michael S. Virk, Yotam Sagi, Lucian Medrihan, Jenny Leung, Michael G. Kaplitt and Paul Greengard

SI Materials and Methods

Antibodies: 5-HT1A (Millipore, AB15350, 1:700), 5-HT1B (Thermo Scientific, PA1-20650 IHC: 1:500; WB: 1:1000), 5-HT5A (Lifespan biosciences inc., LS-A2119, 1:500), 5-HT7 (Abcam, 10913, 1:500). Generic drugs were ordered from Sigma (St. Louis, USA).

Perforated-patch recordings

For perforated-patch recording 3 to 4 week old mice were used for all experiments. After euthanasia with CO2 (Euthanex Smartbox™, USA) the brain was dissected, blocked, and mounted in a vibratome chamber (Vibratome 1000 Plus; Leica Microsystems, USA). Coronal slices (300 µm thick) containing the striatum were cut and recorded in an artificial cerebrospinal fluid (aCSF) containing the following (in mM): 126 NaCl, 2.5 KCl, 2.5 CaCl2, 1.2 MgCl2, 1.2 NaH2PO4, 21.4 NaHCO3, and 11 d-glucose (while being continuously equilibrated with 95% O_2/5% CO_2). Slices were incubated for a minimum of 1 h then transferred to the recording chamber (0.5 ml), and superfused with aCSF (35°C at 1.5 ml/min). For perforated-patch recordings, pipettes (~3-4 MΩ) were front-filled with amphotericin-free internal solution and back-filled with 2-3 µl of internal solution containing amphotericin B (0.5mg/mL) and (in mM): potassium gluconate 136.5, KCl 17.5, NaCl 9, MgCl2 1, HEPES 10, EGTA 0.2, pH 7.20. Following seal formation (> 1 GΩ) with the identified cholinergic neurons in vST or dST the series resistance (Rs) was carefully monitored for any sharp drops (to Rs ~ 10-30 MΩ) as this may indicate a rupture of the membrane to whole-cell configuration. A final, stable Rs was usually reached after 30-45 minutes and lasted for approximately 1 h, during which the recordings were performed. Serotonin and all other drugs were applied directly in the perfusion system. Data were recorded with a Multiclamp 700B/Digidata 1440 system

(Molecular Devices, USA), collected with PowerLab (Chart version 4.2.3) and sampled at 10 kHz.

Stereotaxic injections and optogenetic recordings

AAV9 coexpressing YFP and E123T/H134R channel rhodopsin was injected to the nucleus accumbens of mice 8 and 12 weeks of age. Coordinates were +1.13, +1.10 and -4.82 mm lateral, anterior and ventral relative to Bregma, according to the Franklin and Paxinos Mouse Brain atlas (3rd edition). One week after the injection, mice were euthanized with CO2. After decapitation and brains removal, coronal slices containing nucleus accumbens (300 µm thickness) were cut using a Vibratome 1000 Plus (Leica Microsystems, USA) at 0-4°C in a NMDG-containing cutting solution (in mM): 105 NMDG (N-Methyl-D-glucamine), 105 HCl, 2.5 KCl, 1.2 NaH2PO4, 26 NaHCO3, 25 Glucose, 10 MgSO4, 0.5 CaCl2, 5 L-Ascorbic Acid, 3 Sodium Pyruvate, 2 Thiourea (pH was around 7.4, with osmolarity of 295–305 mOsm). After cutting, slices were left to recover for 15 minutes in the same cutting solution at 35 °C and for 1 h at room temperature (RT) in recording solution. Whole-cell patch-clamp recordings were performed with a Multiclamp 700B/Digidata1550A system (Molecular Devices, Sunnyvale CA, USA) under an upright Olympus BX51WI microscope equipped with the appropriate filters (Olympus, Japan). The extracellular solution used for recordings contained (in mM): 125 NaCl, 25 NaHCO3, 2.5 KCl, 1.25 NaH2PO4, 2 CaCl2, 1 MgCl2 and 25 glucose (bubbled with 95% O_2 and 5% CO_2). The slice was placed in a recording chamber (RC-27L, Warner Instruments, USA) and constantly perfused with oxygenated aCSF at 24 °C (TC-324B, Warner Instruments, USA) at a rate of 1.5–2.0 ml/min. Whole-cell patch-clamp recordings were obtained from spiny projections neurons (SPNs) in the nucleus accumbens. SPNs were identified initially based on their small size and subsequently on their physiological properties (membrane potential around -70 mV and no spontaneous firing). Spontaneous IPSCs were recorded in SPNs in the presence of CNQX and AP5 (to block glutamatergic transmission) in a Cl-rich internal solution (in mM): 126 KCl, 4 NaCl, 1 MgSO4, 0.02 CaCl2, 0.1 BAPTA, 15 Glucose, 5 HEPES, 3 ATP and 0.1 GTP in which the pH was adjusted to 7.3 with KOH and osmolarity was adjusted to 290 mOsmol/l with sucrose. Field light stimulation of

ChETA-expressing cholinergic neurons was done through a 40x objective using a SPECTRA X LED light engine (Lumencor, OR, USA). Data were acquired at a sampling frequency of 50 kHz and filtered at 1 kHz and analyzed offline using pClamp10 software (Molecular Devices, Sunnyvale, CA, USA).

mRNA expression analysis

6 striata from 3 mice were pooled per each translating ribosome affinity purification sample from fresh brains of *ChAT* ^{BacTRAP} (DW-167) mice. To separate the dorsal and ventral striatum, brains were briefly chilled with PBS and coronal cuts were made at the optic chiasm and caudal to the olfactory bulbs. A third coronal cut at the midline of the slab divided the striatum to rostral and caudal sections, and a horizontal cut was made ventrally to the anterior commissure. The dorsal portion of the caudal slice and the ventral part of the rostral slice were used for dorsal and ventral striatum, respectively. RNA isolation, reverse transcription, cDNA amplification and qPCR were done as previously described (1, 2).

Immunohistochemistry

Mouse perfusion and tissue processing were carried out as described (1). For immunostaining of 5-HT1A, 5-HT5A and 5-HT7, *ChAT*^{Cre} *; ROSA26*^{Tdtomato} mice were used to identify ChIs by direct fluorerscence. Under basal conditions, 5-HT1B levels were not detected in the striatum, as previously published (3). For detection and determination of 5-HT1B in ChIs, *ChAT*^{EGFP} (GH-293) mice were intracerebrovascularly infused with 15 µg of colchicine 48 hours prior to the intracardial perfusion to inhibit the axonal transport of 5-HT1B. Four coronal sections of 45 µm thick were stained per antibody per mouse. The mean pixel value of the 5-HTR labeling was determined using image-J in every striatal ChI in the section. ChIs ventral to the anterior commissure were considered ventral striatum (14 ± 3.2 ChIs per section) and ChIs dorsal to the anterior commissure were considered dorsal striatum (82 ± 9.3 ChIs per section). Cells with 5-HTR mean pixel value above 140% of the background were considered immunopositive.

Microdialysis

Guide cannula (CXSG-4, Eicom USA, CA) was placed under general anesthesia and mounted to the skull using Metabond cement (Parkell, Edgewood, NY), and a dummy probe was inserted. The coordinates for the cannula tip were +1.30, +1.10 -3.15 (L,A,V) mm from Bregma for vSt and +2.01, +0.02, -2.34 mm from Bregma for dSt. After recovery of 7-10 days, the animal was anesthetized using 2% Isoflurane. 2 mm long concentric probe (outer diameter of the membrane was 0.22 mm) was slowly lowered to extend directly from the cannula tip (CX-I-4-2, Eicom- USA, CA). The animal was then returned to its home cage with free access to food and water. Dialysis started using solutions that were warmed to 35-37ºc immediately before use. Prior to its insertion, a recovery test was performed for each probe using ACh standard at a flow of 1 µl/ min, using pump controller (BASi inc., IN). Probes with a recovery rate of 15 ± 3.3% (129 / 135 mice) were included. After the placement of the probe, aCSF (Harvard Apparatus, MA) was dialyzed and dialysate fractions were automatically collected (BASi). TTX (10 µM) or calcium free aCSF (140 NaCl, 3.0 KCl, 1.27 $MgCl_2$, 0.27 Na_2HPO_4, 7.2 glucose, all in nM, pH 7.4), were used in some experiments. At the end of the dialysis session the probe was disconnected from the tubing. The animal was immediately euthanized and the position of the probe in the dSt or vSt was visually confirmed (123 / 129 mice were included). ACh content was detected using HPLC-ECD system with AC-GEL separation column (2.0 ID X 150 mm) with a platinum working electrode (all from Eicom-USA, CA). The applied potential was 450 mV and the background current was 5.0-15.4 nA for all samples. Mobile phase consisted of 50 mM KHCO3, 135 µM EDTA-2Na, and 1.6 mM sodium 1-decanesulfonate obtained retention time of 12.9 ± 0.33 min. ACh content in each dialysate sample was determined using subsequent standards with known amounts of ACh. The threshold for detection was 2.44 fmol /min ACh (calculated as 0 fmol + 2*SD).

Neostigmine was added to the diaysis solution since preliminary experiments failed to establish continuous ACh efflux in its absence. 1 µM neostigmine was used in most experiments since doses less than 5 µM do not induce autoinhibiton of ACh release, as previously suggested (4). For each mouse, 20 consecutive 3- minute long dialysates

were collected. Data from mice with ACh level above threshold in all of their 7^{th} – 12^{th} dialysates were included for analysis (72 /123). For each mouse, ACh content from fractions 7^{th} -12^{th} was averaged and was used for statistical analysis.

Animal Behavioral Assays

All the behavioral tests were performed and analyzed by experimenters unaware of the genotype of the animals. For some behavioral tests with the exception of social approach, cohorts of animals were used for multiple tests with the following order: Cookie test, sucrose preference test, novelty suppressed feeding, tail suspension test and forced swim test, with at least 24 hours of interval between tests. SPT, NSF, TST and FST were performed as previously described (5-7).

Cookie Test

The paradigm was adopted from Surget et al., and Isingrini et al.,(8, 9). Mice were familiarized with a daily chocolate cookie in their home cage, for 5 days followed by 5 days without cookie. The test used an apparatus of three aligned compartments with the same dimensions (20 x 20 x 20 cm). Only the colors of the walls and the floor were different between the compartments. The test started by placing a small amount (2 ±1 g) of chocolate fudge stripe mini Keebler cookie in the center of the third (black) compartment. The mouse was placed in the first (white) compartment of the apparatus. The door separating the departure chamber and the intermediate (grey) chamber was closed after the first transition of the mouse. The test was videotaped and variables were measured offline with the exception of number of bites. The latency to pass the first door was measured as well as number of passage through the second door. The latency to take the first bite and the number of bites were recorded within the 10 min test period. The test was performed every other day for a total of four sessions. No effect of session number was found and means of the 4 trials were used for statistical analysis.

Social Approach Test

The paradigm was modified from Launder et al., and Nadler et al. (10, 11). The subject mouse was allowed to freely explore a 3-chamber-arena (58.4 cm x 42.6 cm x 23.1 cm) containing two empty wire mesh cup for 10 minutes. Then, an unfamiliar mouse (male of the same age and fur color) was placed inside a cup on one chamber, and a lego object was placed inside another identical cup in the opposite compartment. The subject mouse was placed in the middle compartment and allowed to freely explore the cups for 10 min. Video tracking software (Ethovision XT7, Noldus, VA) was used to record the session. Social approach was defined by contact between the snout of the subject mouse and the wire mesh cup. The total duration as well as the number of interactions with the unfamiliar mouse and the lego object were scored offline.

Fig. S1

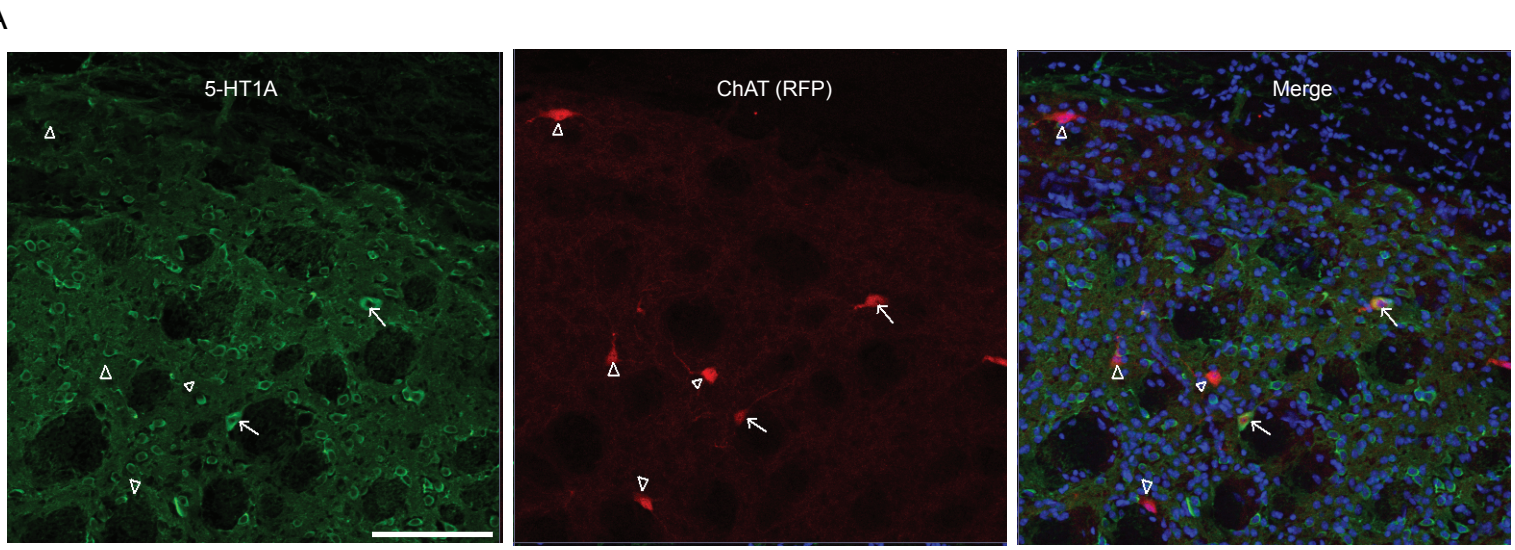
A
5-HT1A
ChAT (RFP)
Merge

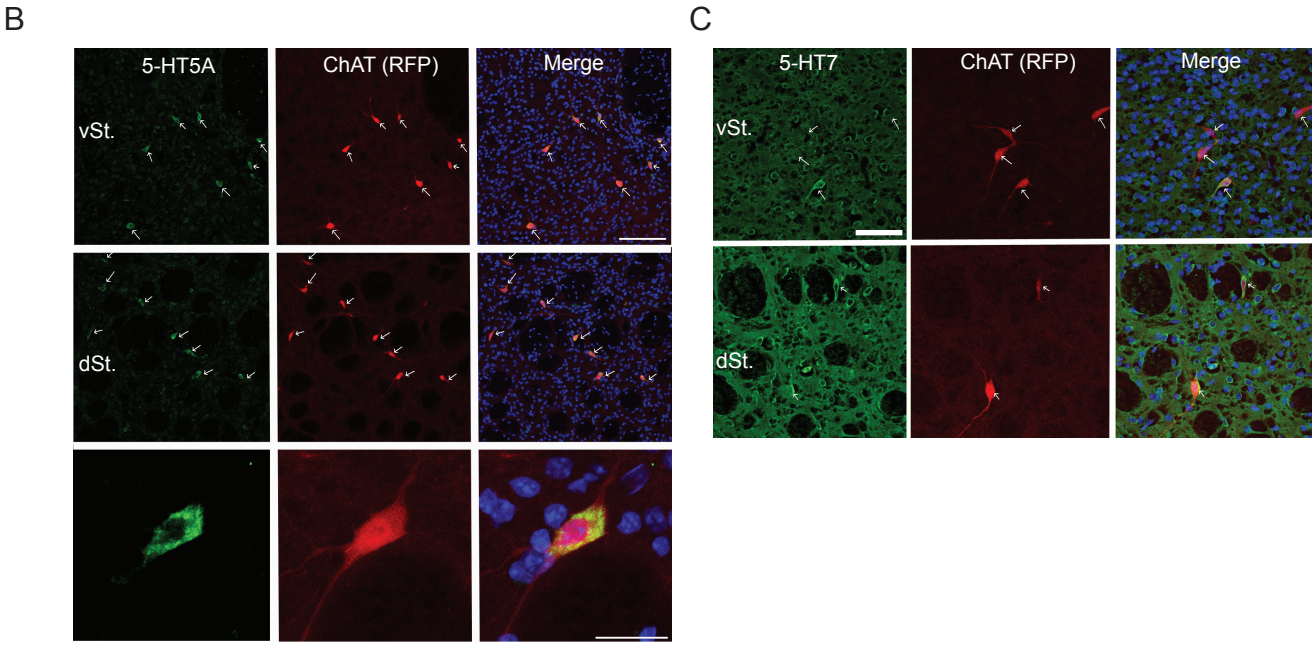
B
5-HT5A
ChAT (RFP)
Merge
vSt.
dSt.
C
5-HT7
ChAT (RFP)
Merge
vSt.
dSt.

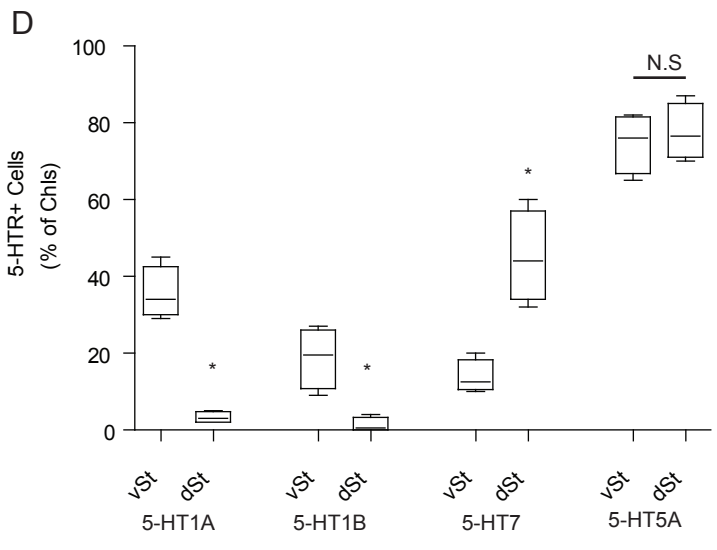
D
5-HTR+ Cells
(% of ChIs)
100
80
60
40
20
0
N.S
*
*
*
vSt
dSt
vSt
dSt
vSt
dSt
vSt
dSt
5-HT1A
5-HT1B
5-HT7
5-HT5A

Fig. S2

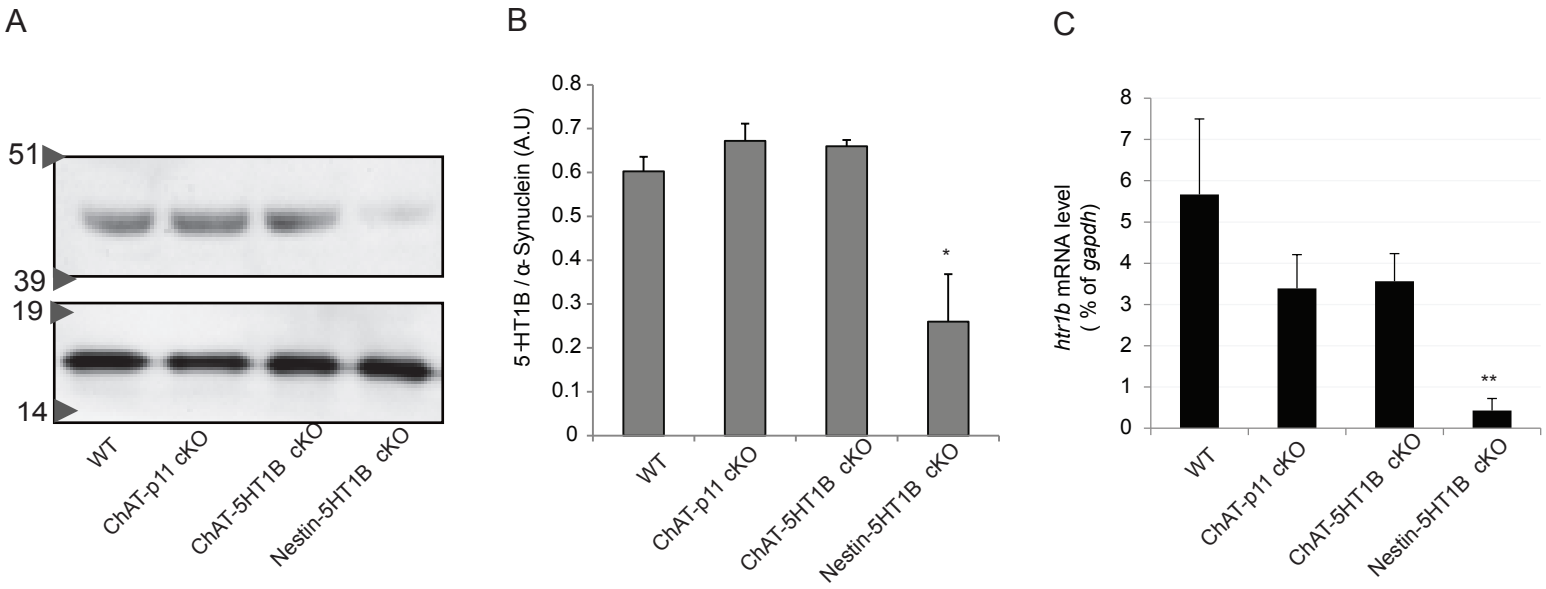
A
51
39
19
14
WT
ChAT-p11 cKO
ChAT-5HT1B cKO
Nestin-5HT1B cKO
B
5-HT1B / α-Synuclein (A.U)
0.8
0.7
0.6
0.5
0.4
0.3
0.2
0.1
0
*
WT
ChAT-p11 cKO
ChAT-5HT1B cKO
Nestin-5HT1B cKO
C
htr1b mRNA level
(% of gapdh)
8
7
6
5
4
3
2
1
0
**
WT
ChAT-p11 cKO
ChAT-5HT1B cKO
Nestin-5HT1B cKO

Fig. S3

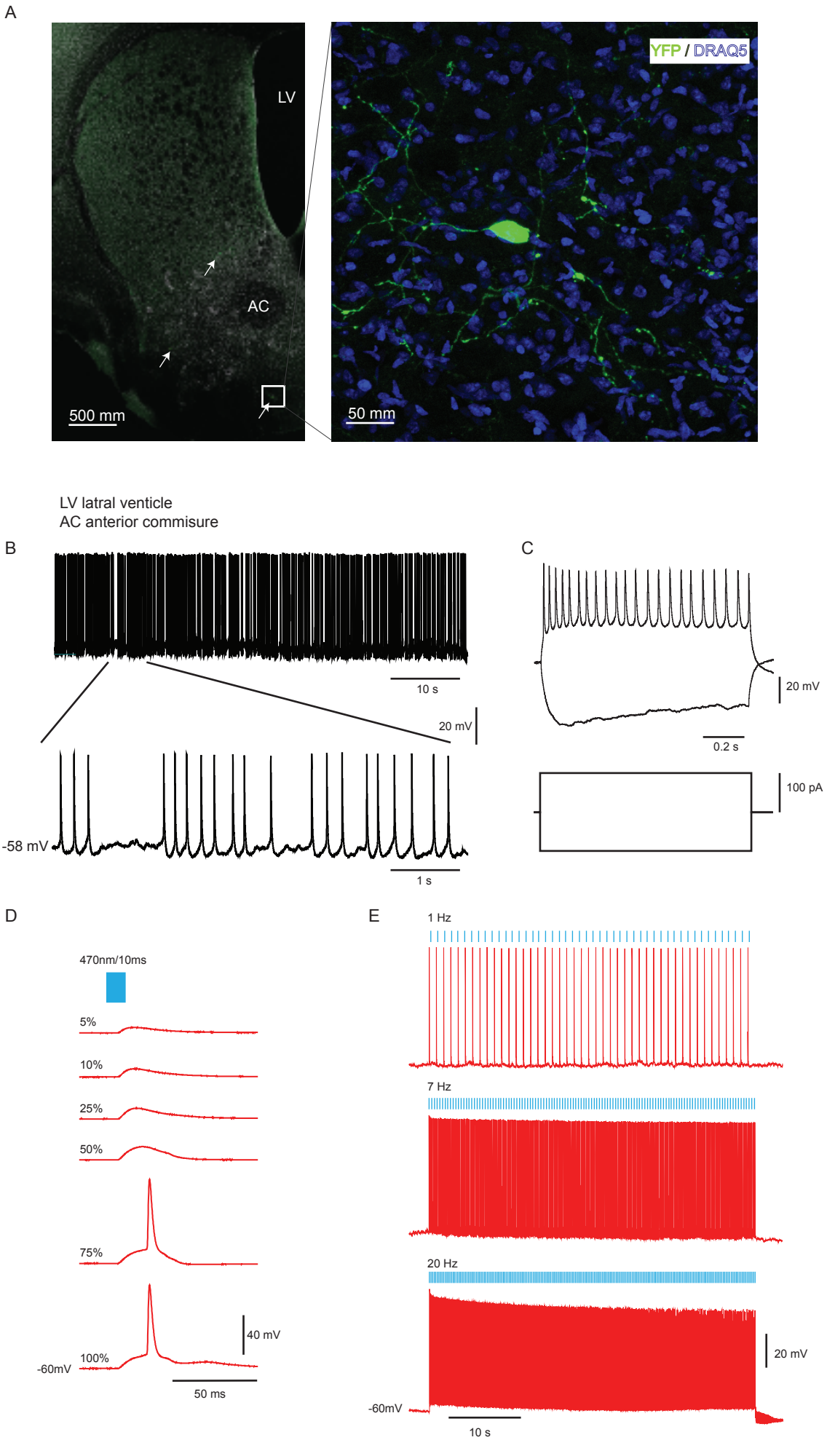
A
LV
AC
500 mm
YFP / DRAQ5
50 mm
LV latral venticle
AC anterior commisure
B
10 s
20 mV
-58 mV
1 s
C
20 mV
0.2 s
100 pA
D
470nm/10ms
5%
10%
25%
50%
75%
100%
-60mV
40 mV
50 ms
E
1 Hz
7 Hz
20 Hz
20 mV
-60mV
10 s

Fig. S4

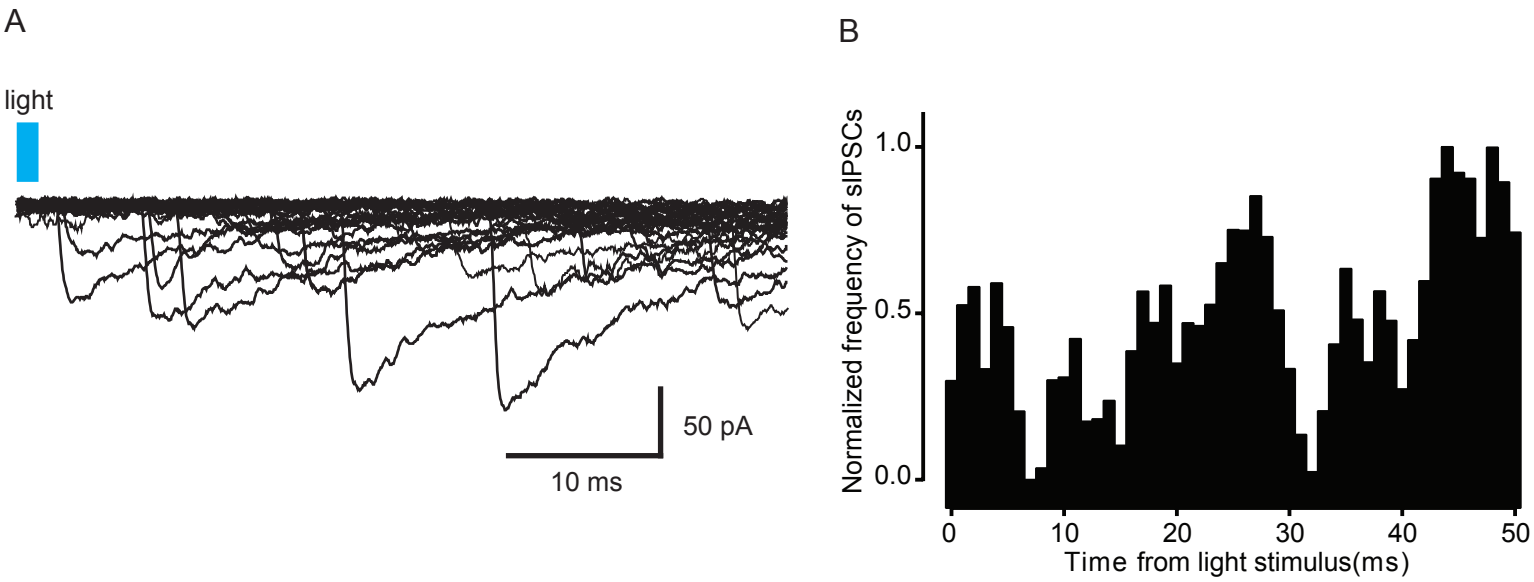
A
light
50 pA
10 ms
B
Normalized frequency of sIPSCs
1.0
0.5
0.0
0
10
20
30
40
50
Time from light stimulus(ms)

Fig. S5

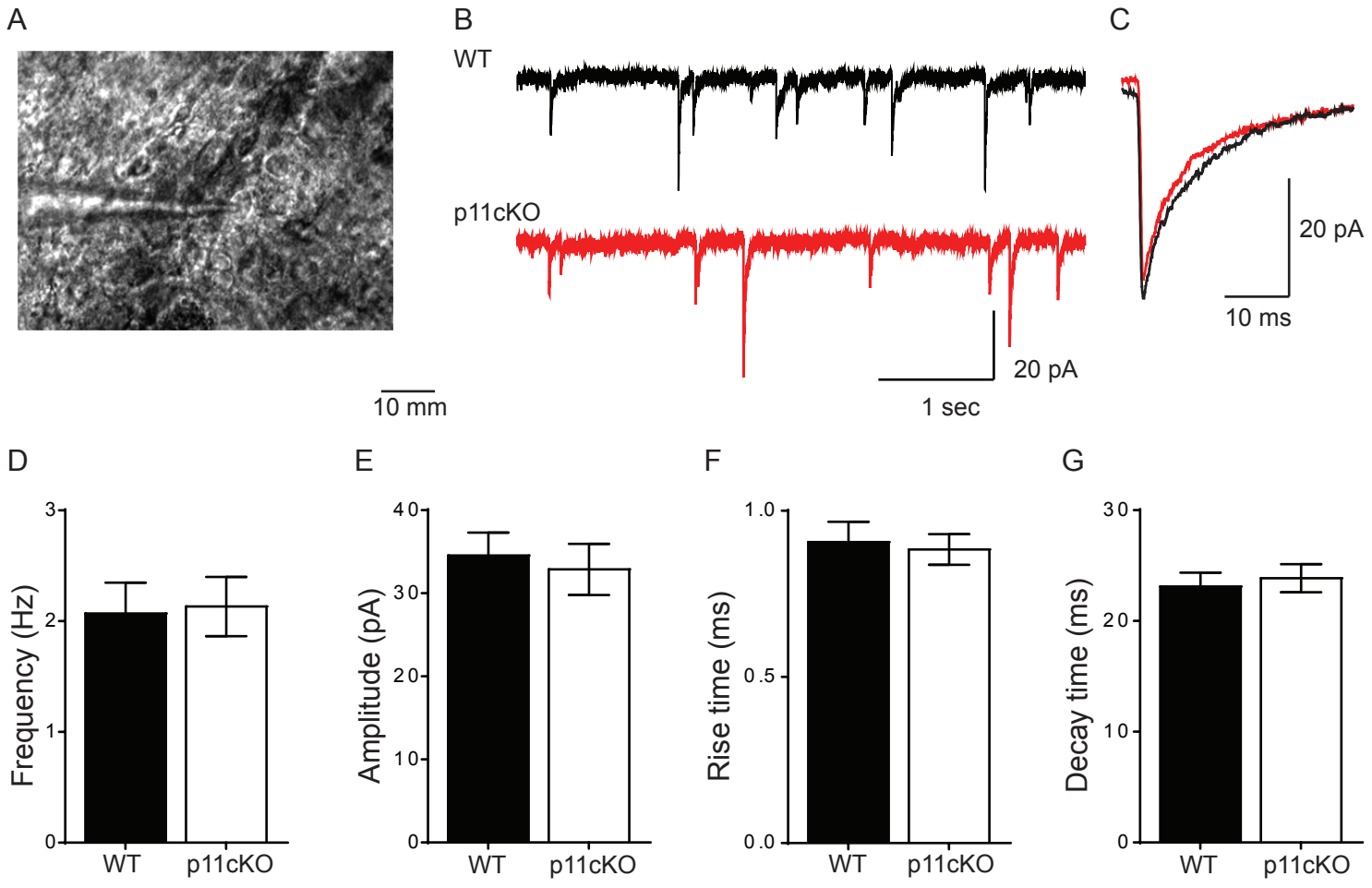
A
B
C
WT
p11cKO
20 pA
10 ms
10 mm
20 pA
1 sec
D
E
F
G
Frequency (Hz)
Amplitude (pA)
Rise time (ms)
Decay time (ms)
WT
p11cKO

Fig. S6

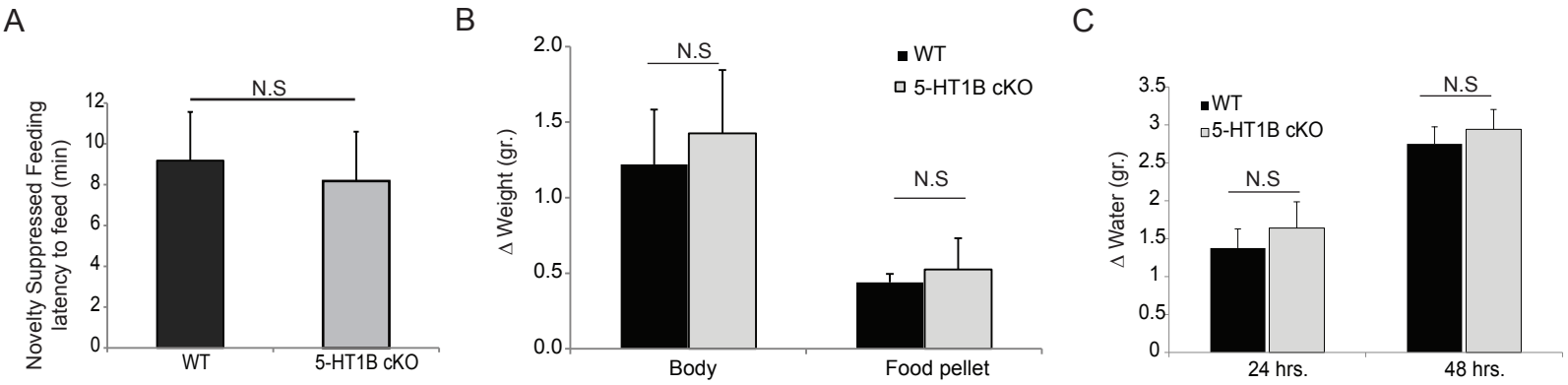
A
Novelty Suppressed Feeding latency to feed (min)
12
10
8
6
4
2
0
N.S
WT
5-HT1B cKO
B
Δ Weight (gr.)
2.0
1.5
1.0
0.5
0.0
N.S
N.S
WT
5-HT1B cKO
Body
Food pellet
C
Δ Water (gr.)
3.5
3
2.5
2
1.5
1
0.5
0
N.S
N.S
WT
5-HT1B cKO
24 hrs.
48 hrs.

Legends for Supplemental Figures

Fig. S1. (*A*) Magnified immonulabeling images of 5-HT1A in the dSt. Note that in dSt, 5HT1A is expressed in some (indicated by arrows) but not in all ChIs (indicated by arrowheads). Scale bars: 100 µm. (*B*) Representative immunolabeling images of 5-HT5A in the ventral and dorsal striatum of $ChAT^{Cre}$;$ROSA26^{Tdtomato}$. Scale bars: 100 µm, 20 µm. (*C*) Representative immunolabeling images of 5-HT7 in the ventral and dorsal striatum of *$ChAT^{Cre}$; $ROSA26^{Tdtomato}$.* Scale bar: 100 µm. (*D*) Box and whiskers plot analysis of the immunolabeling data presented in Fig. 2*A*, *B* and in Fig. S1*B*,*C*, (n= 4 samples per group, * *P*< 0.05 vs. vSt ChIs. N.S, not significant).

Fig. S2. vSt 5-HT1B levels in ChAT-Cre/5-HT1B cKO. (*A*). Representative Western Blot images depicting endogenous 5-HT1B (top) and α-synuclein (bottom) protein levels in vSt lysates from wild type mice (WT) or mice with: null p11 in cholinergic neurons (ChAT-p11 cKO), null 5-HT1B in cholinergic neurons (ChAT- 5-HT1B cKO) or null 5-HT1B in neurons (Nestin-5-HT1B cKO). (*B*) Bar graph summary of the data presented in (*A*). Bars represent mean 5-HT1B levels normalized to α-synuclein ± SD (n=3 mice per group, **P*= 0.02 vs. WT by analysis of variance with *post hoc* two-tailed unpaired *t*-test). (*C*) Bar graph summary of mRNA levels of vSt *htr1b* (n=3 mice per group, ***P*= 0.002 vs. WT by analysis of variance with *post hoc* two-tailed unpaired *t*-test). Note that the level of *htr1b* is lower in the striatum from Nestin-5-HT1B cKO relative to WT but not in that from ChAT 5-HT1B cKO, further supporting the TRAP results that in the striatum, cells other than ChIs express high levels of *htr1b*. Bars represent mean mRNA levels normalized to *gapdh*, as percentage of that in WT ± SD.

Fig. S3. Optogenetics in vSt ChI neurons. (*A*) Representative images of ChIs from the vSt expressing AAV9 with E123T/H134R-ChR2-eYFP. (*B*,*C*) Whole-cell current-clamp recording from eYFP- expressing ChI showing the robust firing characteristic of these cells (*B*) and the specific response to 100 pA current injections (*C*). (*D*) Single stimulus light stimulation of ChIs induced action potentials with the increase in the intensity of the stimulus. (*E*) Light stimulation of ChIs at different stimulation frequencies and 100 %

stimulation intensity showing that trains of action potentials can be elicited at 20 Hz in these cells.

Fig. **S4**. Asynchronous IPSCs in SPNs in response to light stimulation of ChR2 expressing vSt ChIs. (*A*) Traces from an example SPN neuron following each light stimulus within a 20 Hz train showing that IPSCs onset is not coupled synchronously to the stimuli onset. (*B*) Normalized distribution of IPSCs frequency in the 50 ms interval following the onset of all light stimuli in a 20 Hz train in one SPN.

Fig. S5. Spontaneous inhibitory postsynaptic currents in SPNs from vSt. (*A*) Image of a whole-cell patch-clamped SPN in the vSt. (*B*) Representative traces of sIPSC from SPNs in WT and p11cKO mice recorded in the presence of 10 μM CNQX and 10 μM AP5 to block glutamatergic synaptic transmission. (*C*) Average of sIPSCs from one representative SPN from WT and p11 cKO, respectively. (*D*-*G*) Histograms showing no difference in the frequency (*E*), amplitude (*F*) or kinetic properties (*F*, *G*) of sIPSCs between SPNs in WT and p11 cKO (n = 25 for WT and n = 19 neurons for cKO).

Fig. S6. 5-HT1B cKO mice show no deficit in the Novelty Suppressed Feeding test. (*A*) Bar graph represents the latency to feed (mean ± SD; WT=16; cKO, n=18 mice). (*B*) Bar graph summary (mean ± SEM) of the decrease in the weights of the mouse and the food pellet during the test (N.S., not significant). (*C*) Bar graph summary (mean ± SEM) of water consumption during the sucrose preference test (WT, n=13; cKO, n=15 mice; N.S., not significant)

	WT		p11 cKO	
	vSt	**dSt**	**vSt**	**dSt**
ΔRMP in 5-HT (mV)	-5.2 ± 0.71 (n=33)	2.7 ± 0.23 (n=18)	-4.5 ± 0.52^{ns} (n=28)	2.6 ± 0.31^{ns} (n=10)
Δ Firing frequency in 5-HT (Hz)	-0.8±0.67 (n=14)	1.2±0.27 (n=10)	-0.5 ± 0.11^{ns} (n=18)	1.6 ± 0.62^{ns} (n=5)

Table S1.
Summary of the changes in resting membrane potential (ΔRMP-upper row) and firing frequency (lower row) in ChIs following application of 30 μM 5-HT. ns = not significant.

References

1. **Sagi Y, *et al.* (2014) Nitric oxide regulates synaptic transmission between spiny projection neurons. *Proc Natl Acad Sci U S A* 111(49):17636-17641.**
2. **Heiman M, Kulicke R, Fenster RJ, Greengard P, & Heintz N (2014) Cell type-specific mRNA purification by translating ribosome affinity purification (TRAP). *Nat Protoc* 9(6):1282-1291.**
3. **Ghavami A, *et al.* (1999) Differential addressing of 5-HT1A and 5-HT1B receptors in epithelial cells and neurons. *J Cell Sci* 112 (Pt 6):967-976.**
4. **Oldford E & Castro-Alamancos MA (2003) Input-specific effects of acetylcholine on sensory and intracortical evoked responses in the "barrel cortex" in vivo. *Neuroscience* 117(3):769-778.**
5. **Svenningsson P, *et al.* (2006) Alterations in 5-HT1B receptor function by p11 in depression-like states. *Science* 311(5757):77-80.**
6. **Egeland M, Warner-Schmidt J, Greengard P, & Svenningsson P (2010) Neurogenic effects of fluoxetine are attenuated in p11 (S100A10) knockout mice. *Biol Psychiatry* 67(11):1048-1056.**
7. **Warner-Schmidt JL, *et al.* (2012) Cholinergic interneurons in the nucleus accumbens regulate depression-like behavior. *Proc Natl Acad Sci U S A* 109(28):11360-11365.**
8. **Surget A, *et al.* (2011) Antidepressants recruit new neurons to improve stress response regulation. *Mol Psychiatry* 16(12):1177-1188.**
9. **Isingrini E, *et al.* (2010) Association between repeated unpredictable chronic mild stress (UCMS) procedures with a high fat diet: a model of fluoxetine resistance in mice. *PLoS One* 5(4):e10404.**
10. **Landauer MR & Balster RL (1982) A new test for social investigation in mice: effects of d-amphetamine. *Psychopharmacology (Berl)* 78(4):322-325.**
11. **Nadler JJ, *et al.* (2004) Automated apparatus for quantitation of social approach behaviors in mice. *Genes Brain Behav* 3(5):303-314.**